HHS Public Access

Author manuscript

Circ Res. Author manuscript; available in PMC 2018 November 30.

Published in final edited form as:

Circ Res. 2016 September 02; 119(6): 718–730. doi:10.1161/CIRCRESAHA.116.308689.

AMP-Activated Protein Kinase Alpha 2 Deletion Induces VSMC Phenotypic Switching and Reduces Features of Atherosclerotic Plaque Stability

Ye Ding[1], **Miao Zhang**[2], **Wencheng Zhang**[3], **Qiulun Lu**[1], **Zhejun Cai**[1], **Ping Song**[1], **Imoh Sunday Okon**[1], **Lei Xiao**[1], and **Ming-Hui Zou**[1]

[1]Center of Molecular and Translational Medicine, Georgia State University, 100 Piedmont Avenue, Atlanta, GA, 30303, USA

[2]Department of Medicine, University of Oklahoma Health Sciences Center. 941 Stanton L. Young Blvd. Oklahoma City, OK 73104, USA

[3]The Key Laboratory of Cardiovascular Remodeling and Function Research, Chinese Ministry of Education and Chinese Ministry of Health; The State and Shandong Province Joint Key Laboratory of Translational Cardiovascular Medicine, Qilu Hospital of Shandong University, Jinan, China.

Abstract

Rationale: AMP-activated protein kinase (AMPK) has been reported to play a protective role in atherosclerosis. However, whether or not AMPKα2 controls atherosclerotic plaque stability remains unknown.

Objective: The aim of this study was to evaluate the impact of AMPKα2 deletion on atherosclerotic plaque stability in advanced atherosclerosis at the brachiocephalic arteries (BA) and to elucidate the underlying mechanisms.

Methods and Results: Features of atherosclerotic plaque stability and the markers for contractile or synthetic vascular smooth muscle cell (VSMC) phenotypes were monitored in the BA from $Apoe^{-/-}AMPK\alpha2^{-/-}$ mice *or* VSMC-specific $AMPK\alpha2^{-/-}$ mice in an $Apoe^{-/-}$ background ($Apoe^{-/-}AMPK\alpha2^{sm-/-}$) fed western diet for 10 weeks. We identified that $Apoe^{-/-}AMPK\alpha2^{-/-}$ mice and $Apoe^{-/-}AMPK\alpha2^{sm-/-}$ mice exhibited similar unstable plaque features, aggravated VSMC phenotypic switching and significant upregulation of Kruppel-like factor 4 (KLF4) in the plaques located in the BA compared to those found in $Apoe^{-/-}$ *and* $Apoe^{-/-}AMPK\alpha2^{sm+/+}$ control mice. Pravastatin, an AMPK activator, suppressed VSMC phenotypic switching and alleviated features of atherosclerotic plaque instability in $Apoe^{-/-}AMPK\alpha2^{sm+/+}$ mice, but not in $Apoe^{-/-}AMPK\alpha2^{sm-/-}$ mice. VSMC isolated from $AMPK\alpha2^{-/-}$ mice displayed a significant reduction of contractile proteins(SM α-actin, calponin and SM-MHC) in parallel with increased detection of synthetic proteins (vimentin and osteopontin) and KLF4, as observed in

Address correspondence to: Dr. Ming-Hui Zou, Center of Molecular and Translational Medicine, Georgia State University, Piedmont Avenue NE, GA 30303, Atlanta, Tel: 404-413-6637, mzou@gsu.edu.

DISCLOSURES

None.

vivo. KLF4-specific siRNA abolished AMPKα2 deletion-induced VSMC phenotypic switching. Further, pharmacological or genetic inhibition of NF-κB significantly decreased KLF4 upregulation in VSMC from *AMPKα2*$^{-/-}$ mice. Finally, we found AMPKα2 deletion markedly promoted the binding of NF-κBp65 to KLF4 promoter.

Conclusions: This study demonstrated that AMPKα2 deletion induces VSMC phenotypic switching and promotes features of atherosclerotic plaque instability in NF-κB-KLF4 dependent manner.

Keywords

AMPK; KLF4; VSMC phenotypic switching; plaque instability; AMP-activated protein kinase signal transduction; atherosclerosis; vulnerable plaque; vascular smooth muscle

Subject Terms:

Atherosclerosis; Coronary Artery Disease; Vascular Disease

INTRODUCTION

Atherosclerosis, characterized by the accumulation of lipids and inflammatory cells in the large arteries, is one of the most common causes of morbidity and mortality in developed and developing countries[1, 2]. Atherosclerotic plaque rupture-induced thrombosis or obstruction of coronary artery is the most important cause for the sudden and unpredictable onset of acute coronary syndromes[3]. Vulnerable plaques have thin fibrous caps and contain reduced collagen contents. VSMC, which are able to form and maintain the fibrous cap as well as synthesize collagen[4], play a pivotal role in enhancing plaque stability in advanced lesions. Most studies of the role of VSMC on atherosclerotic plaque stability are focused on VSMC apoptosis[5, 6]. It has been shown that apoptosis of VSMC induces features of plaque vulnerability in atherosclerosis[7]. However, recently, Owens et al. reported that the contribution of VSMC to atherosclerotic plaques has been greatly underestimated, and KLF4-dependent transitions in SMC phenotype are critical in lesion pathogenesis[8]. Using VSMC-specific KLF4 knockout mice, they identified that KLF4 deletion increases multiple indices of plaque stability, suggesting that therapeutic approaches aimed at reducing KLF4 may be a viable means of treating advanced atherosclerosis. But how KLF4 itself is regulated in atherosclerosis remains unclear. Over the years, pathogenic factors causing atherosclerotic plaque instability have been a subject of intensive investigation.

AMP-activated protein kinase (AMPK) is a serine/threonine kinase composed of α, β, and γ subunits[9, 10]. The α subunit which controls catalytic activity, has two isoforms, α1 and α2, which are differentially expressed in various cell types[11, 12]. All three major cell types in the vasculature (endothelial cells, VSMC, and monocytes/macrophages) express AMPKα. The major isoform in these vasculature cells is AMPKα1 where as AMPKα2 is the minor isoform. Despite being the minor isoform, AMPKα2 plays an important role in cardiovascular diseases. Recent studies indicate that AMPK not only functions as an intracellular energy sensor and regulator[13, 14], but also plays critical roles in the pathogenesis of several cardiovascular diseases[15, 16]. For example, genetic deletion of

AMPKα2 in endothelial cells accelerates atherosclerosis by promoting NAD(P)H oxidase, reactive oxygen species (ROS), endothelial dysfunction, and endoplasmic reticulum (ER) stress[17, 18]. Additionally, AMPKα2 deletion in VSMC promotes neointimal formation by enhancing VSMC migration and proliferation[19, 20]. But the contributions of VSMC-derived AMPKα2 in atherosclerosis and plaque stability remains unknown.

By using loss-of-function approach (global $AMPK\alpha2^{-/-}$ and VSMC-specific $AMPK\alpha2^{-/-}$ mice) and activation of AMPKα2 by pravastatin, we aimed to determine the effect and molecular mechanisms of AMPKα2 on atherosclerosis and atherosclerotic plaque stability. Our results indicate that AMPKα2 deletion in VSMC promotes features of atherosclerotic plaque instability via upregulating KLF4 expression. Conversely, pravastatin suppressed VSMC phenotypic switching and enhanced plaque stability via AMPKα2 activation.

METHODS

Animal diet, feeding schedule and preparation of tissues.

Male $Apoe^{-/-}$ and $Apoe^{-/-}AMPK\alpha2^{-/-}$ mice were fed a western diet containing 21% milk fat and 0.15% cholesterol for 10 weeks starting at 8 weeks of age. Similarly, 8-week old male $Apoe^{-/-}AMPK\alpha2^{sm+/+}$ and $Apoe^{-/-}AMPK\alpha2^{sm-/-}$ mice were placed on western diet for the initial 6 weeks to establish aortic lesions. In the presence of western diet, mice were treated with 50mg/kg/day pravastatin for an additional 4 weeks. Saline solution was used as solvent control. Mice were sacrificed and blood was collected. Mice were then perfused via the left ventricle with 5 ml PBS followed by 10 ml 4% paraformaldehyde. Brachiocephalic arteries (BA) were carefully dissected and fixed overnight in 4% paraformaldehyde prior to embedding in optimum cutting temperature compound (OCT; BDH Laboratory Supplies).

Details of materials and experimental procedures are in the Methods section in the Online Data Supplement.

RESULTS

AMPKα2 deletion enhances features of atherosclerotic plaque instability.

To examine the effects of AMPKα2 deletion on atherosclerotic plaque stability at the BA, we first analyzed the lesion sizes with oil red O staining. Consistent with our previous report[17], $Apoe^{-/-}AMPK\alpha2^{-/-}$ mice exhibited an elevation in atherosclerotic plaque size spanning over 6 locations within the BA compared with those of $Apoe^{-/-}$ controls (Supplemental Figure IA–D).

The phenotypic characteristics of vulnerable plaques include increased intraplaque hemorrhage[21, 22], presence of buried fibrous cap[23, 24], presence of discontinuity in the fibrous cap[25], increased lipid-rich necrotic core size, decreased thickness of fibrous cap[23], decreased plaque collagen content[26, 27], increased macrophage content[28, 29] and increased matrix metallaproteases (MMPs), all of which have been widely used as indicators of plaque instability. To test whether or not AMPKα2 deletion influence the features of plaque stability, the aforementioned parameters were detected within the BA, a widely used artery for studying plaque stability or vulnerability in terms of an advanced atherosclerotic lesion

in a mouse model. Intraplaque hemorrhage (Figure 1A black arrow), defined as the presence of erythrocytes within the plaque, contributes independently to plaque instability as they promote oxidative stress and cholesterol accumulation[30], was significantly increased in *Apoe*$^{-/-}$*AMPKα2*$^{-/-}$ mice relative *to Apoe*$^{-/-}$ mice (Figure 1B); In addition, buried fibrous caps which may represent old plaque ruptures that have healed[24, 31] dramatically increased in *Apoe*$^{-/-}$*AMPKα2*$^{-/-}$ mice compared with that of *Apoe*$^{-/-}$ mice (Figure 1A black arrowhead and 1C). The presence of fibrous cap discontinuity, which also called acute plaque rupture, defined as a visible breach in the cap[32], may directly reflect plaque rupture, and was found increased in *Apoe*$^{-/-}$*AMPKα2*$^{-/-}$ mice (Figure 1D). Furthermore, plaque necrosis, which contributes to inflammation, thrombosis, physical stress on the fibrous cap and plaque breakdown[33], was analyzed and the result showed that the necrotic core size in *Apoe*$^{-/-}$*AMPKα2*$^{-/-}$ mice was significantly increased relative to *Apoe*$^{-/-}$ mice (Figure 1E and 1F). Fibrous cap area, which is widely used as an indirect indicator of plaque stability, was markedly decreased in *Apoe*$^{-/-}$*AMPKα2*$^{-/-}$ mice relative to controls, consistent with features of unstable plaques in humans (Figure 1G and 1H). Also, plaque collagen content, which plays an important structural role in stabilizing plaques[34], was decreased in *Apoe*$^{-/-}$*AMPKα2*$^{-/-}$ mice relative to control mice (Figure 1I and 1J). Additionally, macrophage content was increased within plaques from *Apoe*$^{-/-}$*AMPKα2*$^{-/-}$ mice relative to controls, which is also consistent with increased plaque instability (Figure 1K and 1L). Finally, the expression of MMP2, which is a key factor in promoting the vulnerability of an atherosclerotic plaque, was significantly increased in plaque enriched areas of the BA in *Apoe*$^{-/-}$*AMPKα2*$^{-/-}$ mice relative to control mice (Supplemental Figure II). Taken together, these results demonstrate that AMPKα2 deletion promotes features of an unstable plaque phenotype in advanced atherosclerosis.

AMPKα2 deletion induces VSMC phenotypic switching in vivo.

VSMC phenotypic switching, mostly defined by a decreased expression of contractile genes and an increase in synthetic genes, plays a pivotal role in enhancing atherosclerotic plaque instability in advanced lesions. To examine the effect of AMPKα2 on regulating VSMC phenotypic switching in vivo, we evaluated changes in expression of molecular markers for contractile and synthetic VSMC phenotypes in the BA from *Apoe*$^{-/-}$ and *Apoe*$^{-/-}$*AMPKα2*$^{-/-}$ mice. As observed by Immunohistochemistry (IHC) and Immunofluorescence (IF) imaging, SM α-actin expression, which is a typical marker of contractile VSMC, in both the fibrous caps and total plaque showed significant decrease in *Apoe*$^{-/-}$*AMPKα2*$^{-/-}$ mice relative to *Apoe*$^{-/-}$ controls (Figure 2A, 2B and 2C). While vimentin, which is considered a marker of synthetic VSMC[35], was significantly increased in the *Apoe*$^{-/-}$*AMPKα2*$^{-/-}$ mice compared with the *Apoe*$^{-/-}$ controls (Figure 2D, 2E and 2F). In addition, the expression of SM α-actin and vimentin in the media of BA (in which the major cell type is VSMC) showed similar trend with that in the plaque area. All these results demonstrate that AMPKα2 deletion promotes contractile VSMC switching to the synthetic phenotype, which might lead to plaque instability.

AMPKα2 deletion upregulates KLF4 expression in advanced atherosclerotic plaque in BA.

Kruppel-like factor 4 (KLF4) is a transcription factor of the KLF family and regulates differentiation, proliferation and apoptosis[36]. KLF4 is a well-known negative transcriptional

factor for VSMC contractile proteins, which is reported to be upregulated in VSMC phenotype modulation and plaque instability[8]. We reasoned that AMPKα2 deletion causes increased KLF4 resulting in VSMC phenotypic switching and plaque instability. To this end, we detected KLF4 expression in the plaques of BA from *Apoe*$^{-/-}$ and *Apoe*$^{-/-}$*AMPKα2*$^{-/-}$ mice. As shown in Figure 3A and 3B, KLF4 expression was significantly increased in both the plaque areas and media layer of the vessel (mainly VSMC) in *Apoe*$^{-/-}$*AMPKα2*$^{-/-}$ mice relative to that of *Apoe*$^{-/-}$ mice. To further identify the origin of increased KLF4, IF co-staining of KLF4, SM α-actin and CD68 indicated that there was weak co-staining of KLF4 and macrophage marker CD68 (pink) in the plaque of BA in both *Apoe*$^{-/-}$ and *Apoe*$^{-/-}$*AMPKα2*$^{-/-}$ mice (Supplemental Figure III), suggesting that the major origin of increased KLF4 in *AMPKα2*$^{-/-}$ mice is VSMC. These results indicate that KLF4 might be required for AMPKα2 deletion-induced VSMC phenotypic switching and plaque instability.

VSMC-specific AMPKα2 deletion but not macrophage-specific AMPKα2 deletion exacerbates western diet-induced atherogenesis and plaque instability.

To evaluate the contribution of VSMC in AMPKα2 deletion-induced plaque instability, we generated *Apoe*$^{-/-}$ background VSMC-specific AMPKα2$^{-/-}$ (*Apoe*$^{-/-}$*AMPKα2*$^{sm-/-}$) mice and macrophage-specific AMPKα2$^{-/-}$ (*Apoe*$^{-/-}$*AMPKα2*$^{f/f}$LyzM^{cre}) mice. Western blot analysis confirmed that AMPKα2 was efficiently knocked down in VSMC from the aorta of *Apoe*$^{-/-}$*AMPKα2*$^{sm-/-}$ mice (Supplemental Figure IV). We first evaluated the effects of AMPKα2 in VSMC on atherogenesis in the BA. Oil red O staining showed that atherosclerotic plaque size within the BA of *Apoe*$^{-/-}$*AMPKα2*$^{sm-/-}$ mice was enhanced compared with those of *Apoe*$^{-/-}$*AMPKα2*$^{sm+/+}$ mice (Supplemental Figure V and Figure 4B). Plaque instability indices were analyzed in BA from *Apoe*$^{-/-}$*AMPKα2*$^{sm-/-}$ mice and *Apoe*$^{-/-}$*AMPKα2*$^{sm+/+}$ mice. As depicted in Figure 4A and 4C, *Apoe*$^{-/-}$*AMPKα2*$^{sm-/-}$ mice displayed significantly increased necrotic core size compared with that of *Apoe*$^{-/-}$*AMPKα2*$^{sm+/+}$ mice. In parallel, decreased collagen content and reduced fibrous cap area were evident in *Apoe*$^{-/-}$*AMPKα2*$^{sm-/-}$ mice relative to *Apoe*$^{-/-}$*AMPKα2*$^{sm+/+}$ mice (Figure 4D–F). These results demonstrate that *Apoe*$^{-/-}$*AMPKα2*$^{sm-/-}$ mice exhibit features of plaque instability similar to those in the BA of global *AMPKα2*$^{-/-}$ mice. In contrast, there was no difference in atherosclerotic plaque formation and plaque stability in BA of *Apoe*$^{-/-}$*AMPKα2*$^{f/f}$ control mice and *Apoe*$^{-/-}$*AMPKα2*$^{f/f}$*LyzM*^{cre} mice (Supplemental Figure VI). These results strongly suggest that VSMC-derived AMPKα2 is required for anti-atherogenesis and plaque stabilization.

Pravastatin treatment alleviates western diet-induced plaque instability in Apoe$^{-/-}$AMPKα2$^{sm+/+}$ mice but not in Apoe$^{-/-}$AMPKα2$^{sm-/-}$ mice.

Pravastatin which is widely used for reducing the risk of cardiovascular disease has been reported as an AMPKα2 activator[37]. To test whether or not pravastatin activates AMPK in VSMC, human aortic smooth muscle cells (HASMC) were treated with pravastatin (0.01–50 μM) for 24 hours. Consistent with a previous report in endothelial cells[37], pravastatin caused a dose dependent increase in AMPK phosphorylation at Thr172 in HASMC (Figure 4G). In addition, the Thr172 phosphorylation/activation of AMPK in mouse aorta was observed after 4 weeks of pravastatin administration (Figure 4H). Reactive oxygen species (ROS) has been reported as an upstream signal for AMPK activation[38, 39]. As shown in Supplemental figure

VIIA–E, exposure of HASMC to pravastatin increased ROS and the activation of AMPK by pravastatin was effectively blocked by either Tempol or mito-Tempol, two potent ROS scavengers, suggesting that AMPK activation by pravastatin is ROS mediated.

Pravastatin treatment had no effect on mice body weight (Supplemental Table I) and total plasma cholesterol and triglyceride levels (Supplemental Table II). We had earlier determined whether pravastatin's protective effect on plaque stability was mediated by VSMC-derived AMPKα2. As shown in Figure 4, pravastatin, administrated for 4 weeks, caused a 49% decrease of necrotic core size (Figure 4C), 17% increase of collagen (Figure 4D–E), and 10% increase of fibrous cap thickness (Figure 4F), in $Apoe^{-/-}AMPK\alpha2^{sm+/+}$ mice compared to control. There was a slight decrease in plaque size after treatment with pravastatin, suggesting that pravastatin had little effect on plaque regression. As expected, unlike the effects of pravastatin in $Apoe^{-/-}AMPK\alpha2^{sm+/+}$ mice, pravastatin treatment had no effect on plaque stability, including plaque size, necrotic core size, collagen content and fibrous cap thickness in $Apoe^{-/-}AMPK\alpha2^{sm-/-}$ mice (Figure 4 A–F). These data support the notion that pravastatin enhances plaque stability in the BA via VSMC AMPKα2 signaling.

VSMC AMPKα2 knockdown eliminates the effect of pravastatin treatment on VSMC phenotypic switching signaling in vivo.

We further determined whether VSMC specific AMPKα2 knockdown could induce VSMC phenotypic switching in the BA. As shown in Figure 5A–C, $Apoe^{-/-}AMPK\alpha2^{sm-/-}$ mice exhibited significantly reduced SM α-actin content in both the fibrous cap and total plaque area relative to $Apoe^{-/-}AMPK\alpha2^{sm+/+}$ mice. Conversely, the expression of synthetic marker vimentin was markedly increased in the plaque of $Apoe^{-/-}AMPK\alpha2^{sm-/-}$ mice compared to $Apoe^{-/-}AMPK\alpha2^{sm+/+}$ mice (Figure 5D–F). Meanwhile, we found enhanced KLF4 staining within the BA of $Apoe^{-/-}AMPK\alpha2^{sm-/-}$ mice compared to that in $Apoe^{-/-}AMPK\alpha2^{sm+/+}$ mice, which is consistent with the AMPKα2 global knockout mice (Figure 3). As shown in Figure 5A–H, pravastatin treatment not only markedly down-regulated KLF4 expression in BA, but significantly increased SM α-actin expression and decreased vimentin expression on the plaque cap and in the total plaque of $Apoe^{-/-}AMPK\alpha2^{sm+/+}$ mice. However, pravastatin treatment had no effects on the expression of SM α-actin, vimentin and KLF4 in BA in $Apoe^{-/-}AMPK\alpha2^{sm-/-}$ mice (Figure 5). In addition, the levels of SM α-actin, vimentin and KLF4 in the media of BA of these four group mice displayed similar trend with that in the plaque area (Figure 5). Finally, we observed weak co-staining of KLF4 and CD68 in BA of the mice in these four groups (Supplemental Figure VIIIA). Taken together, these results suggest that VSMC is the major cell origin of KLF4 and that pravastatin via its activation of VSMC AMPKα2 suppresses VSMC phenotypic switching.

VSMC AMPKα2 deficiency does not promote VSMC-to-macrophage phenotypic switching.

Owens et al. demonstrate that KLF4 promotes switching of VSMC to macrophage phenotype in atherosclerotic plaques[8]. Thus, we reasoned that AMPKα2 deficiency may promote VSMC-to-macrophage phenotypic switching by upregulating KLF4. To address this issue, we conducted both in vivo and in cultured VSMC experiments. We first performed IF staining of CD68 and SM α-actin in BA of $Apoe^{-/-}AMPK\alpha2^{sm-/-}$ mice and $Apoe^{-/-}AMPK\alpha2^{sm+/+}$ mice with or without pravastatin. As shown in Supplemental Figure

VIIIB, pravastatin reduced macrophage contents both in *Apoe*$^{-/-}$*AMPKα2*$^{sm+/+}$ mice and *Apoe*$^{-/-}$*AMPKα2*$^{sm-/-}$ mice, indicating that macrophage-lowering effects of pravastatin is AMPKα2 independent. Western diet reduced SM α-actin staining in mouse aortas from *Apoe*$^{-/-}$ mice (data not shown). Interestingly, pravastatin attenuated the reduction of SM α-actin in western diet fed *Apoe*$^{-/-}$ mice but not in *Apoe*$^{-/-}$*AMPKα2*$^{sm-/-}$ mice (Supplemental VIIIB), indicating AMPKα2 activation in VSMC is required for pravastatin's effects on SM α-actin.

We next examined macrophage markers in cultured VSMC under cholesterol loading. As depicted in Supplemental Figure VIIIC, cholesterol loading caused a 2 fold increase of the mRNA levels of macrophage marker lgals3 in both WT and *AMPKα2*$^{-/-}$ VSMC. In addition, under either basal or cholesterol treated conditions, the level of lgals3 in *AMPKα2*$^{-/-}$ VSMC was lower than that of WT VSMC (Supplemental Figure VIIIC), suggesting that loss of AMPKα2 in VSMC unlikely promotes its VSMC switching into macrophage under cultured conditions. Taken together, these results provide further evidence that AMPKα2 deficiency has no direct effect on promoting VSMC-to-macrophage phenotypic switching.

AMPKα2 deficiency induces VSMC phenotypic switching in vitro.

To elucidate the mechanism of AMPKα2 on VSMC phenotypic switching, we isolated VSMC from the aorta of WT and *AMPKα2*$^{-/-}$ mice and detected markers of contractile and synthetic VSMC phenotypes by real-time PCR and western blotting. As shown in Figure 6A, SM α-actin, calponin and SM-MHC, which are three canonical contractile markers of VSMC, were significantly decreased in *AMPKα2*$^{-/-}$ VSMC compared to those from WT. In contrast, the mRNA and protein levels of vimentin and osteopontin, two well-characterized markers for synthetic VSMC, were dramatically increased in *AMPKα2*$^{-/-}$ VSMC (Figure 6A and 6B). Consistently, transfection of AMPKα2-specific siRNA, but not control siRNA, in HASMC not only significantly lowered the amount of contractile proteins (SM α-actin, calponin and SM-MHC) but caused a marked upregulation of synthetic proteins (vimentin and osteopontin) (Figure 6C and 6D). Furthermore, we analyzed the levels of extracellular matrix and MMP2 protein expression and activity in WT or *AMPKα2*$^{-/-}$ VSMC. As we expected, both Collagen I and Collagen IV were increased in *AMPKα2*$^{-/-}$ VSMC compared to those from WT. Consistently, MMP2 expression and MMP2 activity were markedly elevated in *AMPKα2*$^{-/-}$ VSMC when compare to those from WT (Supplemental Figure IXA). Consistently, transfection of AMPKα2-specific siRNA, but not control siRNA, in HASMC significantly increased Collagen I and MMP2 (Supplemental Figure 9B). Taken together, our results indicate that AMPKα2 deletion triggers the switch of contractile VSMC to the synthetic phenotypes in vitro as well as in vivo.

AMPKα2 deficiency upregulates KLF4 in VSMC.

Next, we detected KLF4 protein expression in VSMC isolated from WT and *AMPKα2*$^{-/-}$ mice. As shown in Figure 7A, KLF4 protein was significantly increased in VSMC from *AMPKα2*$^{-/-}$ mice compared to their counterparts from WT. Furthermore, the mRNA levels of KLF4 in the VSMC from *AMPKα2*$^{-/-}$ mice were 2.6 fold greater than those in VSMC from WT (Figure 7B). Similarly, siRNA-knock down of AMPKα2 in HASMC significantly

increased both the mRNA level and protein expression of KLF4 (Figure 7C and 7D). Taken together, these results indicate that genetic inhibition of AMPKα2 in VSMC upregulated KLF4.

KLF4 knockdown ablates AMPKα2 deletion-induced VSMC phenotypic switches in cultured VSMC.

To further investigate a causative role of KLF4 accentuation in AMPKα2 deletion-induced VSMC phenotypic switching, the mRNA and protein expression levels of the contractile and synthetic markers were monitored in VSMC transfected with either KLF4-specific siRNA or con siRNA. As expected, transfection of KLF4-specific siRNA, but not con siRNA, significantly suppressed KLF4 expression in VSMC (Figure 7E). Silencing of KLF4 in *AMPKα2*$^{-/-}$ VSMC prevented the reduction of mRNA and protein levels for contractile markers such as SM α-actin and calponin, as well as prevented upregulation of synthetic markers (Figure 7E and 7F).

To further confirm the involvement of KLF4 in AMPKα2 deletion-induced VSMC phenotypic switching, we concomitantly silenced both KLF4 and AMPKα2 in HASMC. As expected, siRNA-mediated KLF4 silencing rescued the attenuation of contractile markers caused by AMPKα2 deficiency (Figure 7G and 7H). Meanwhile, elevated expression of both protein and mRNA levels of synthetic markers mediated by AMPKα2 silence was blocked in HASMC transfected with KLF4-specific siRNA (Figure 7G and 7H). In summary, our results indicate that KLF4 is required for AMPKα2 deletion-induced VSMC phenotype switching in VSMC.

AMPKα2 deficiency upregulates KLF4 through NF-κB signaling.

Next, we determined whether AMPKα2 deletion activates the NF-κB pathway in VSMC. First we analyzed the protein expression of NF-κB pathway molecular markers in VSMC isolated from WT and *AMPKα2*$^{-/-}$ mice by using western blots. As shown in Supplemental Figure X, the expression of p-IκBα, pNF-κB p65, and NF-κB p65 in the nucleus were significantly increased in *AMPKα2*$^{-/-}$ VSMC relative to VSMC from WT. In addition, *AMPKα2*$^{-/-}$ VSMC showed decreased expression of IκBα indicating enhanced degradation of IκBα in VSMC. These data suggest that AMPKα2 deficiency in VSMC resulted in over activation of NF-κB and consequent KLF4 upregulation. To further study the contributions of the NF-κB pathway in AMPKα2 deletion-mediated KLF4 upregulation, we used a synthetic NF-κB inhibitor which inhibits translocation of the NF-κB active complex into the nucleus, thereby pharmacologically blocking the NF-κB pathway in WT and *AMPKα2*$^{-/-}$ VSMC. Notably, inhibition of NF-κB abolished AMPKα2 deficiency-induced upregulation of KLF4 protein and mRNA levels (Figure 8A and 8B). NF-κB p65 and AMPKα2 were concomitantly silenced in HASMC. As depicted in Figure 8C and 8D, silencing of NF-κB p65 ablated KLF4 upregulation in AMPKα2-silenced HASMC, suggesting that the NF-κB pathway play a critical role in AMPKα2 deficiency-mediated KLF4 upregulation.

Considering that AMPKα2 deficiency upregulates both the mRNA level and protein expression of KLF4, we hypothesized that AMPKα2 deficiency may upregulate KLF4 through transcriptional activation. By using the Transcription Factor Database (http://

www.gene-regulation.com), we found that KLF4's upstream promoter contains a putative NF-κB p65 binding site (tcccagggaagtccct; at 2,018-bp). To confirm the predicted site of the KLF4 promoter is required for increased KLF4 expression in HASMC in response to AMPKα2 deficiency, we constructed two promoter-reporter plasmids containing different lengths of KLF4 promoter (Figure 8E). HASMC were transfected with different KLF4 promoter-reporter plasmids along with con siRNA and AMPKα2 siRNA. Promoter activity was analyzed by luciferase assay. As depicted in Figure 8F, AMPKα2 deficiency increased the activity of the 2,600-bp promoter, however had no effect on the activity of the 1,583-bp promoter, implying that the regulatory element necessary for AMPKα2 deficiency-induced increase in KLF4 expression is located between 1,583-bp to 2,600bp, which is consistent with our prediction.

To directly test if the 2,018-bp predicted site within the KLF4 promoter was responsible for transcriptional regulation by AMPKα2/NF-κB pathway, we performed a promoter assay (luciferase reporter assay) using a KLF4 promoter containing a mutation at 2,018-bp. HASMC were simultaneously transfected with WT or KLF4 mutant 2,018-bp promoter-reporter plasmid along with con siRNA and AMPKα2 siRNA. Mutagenesis analysis of KLF4 promoter showed that deletion of the region that contains the potential NF-κB site (2,018-bp) blocked the increase of the promoter activity induced by AMPKα2 deficiency compared with WT plasmid in HASMC. A significant reduction of KLF4 promoter activity in 1,583-bp construct compared with 2,600-bp was also observed in HASMC **(**Figure 8G).

Finally, we determined the effect of AMPKα2 deficiency on binding activity of NF-κB p65 with the KLF4 promoter. Different primers were designed and DNA Chromatin Immunoprecipitation (ChIP) assays were performed in *AMPKα2*$^{-/-}$ and WT VSMC. As expected, AMPKα2 deletion markedly promoted the binding of NF-κB p65 to the KLF4 promoter (Figure 8H). Taken together, AMPKα2 deletion via NF-κB transcriptional regulation induced KLF4 upregulation.

DISCUSSION

The current study demonstrates for the first time that AMPKα2 plays a novel role as a powerful negative regulator of VSMC phenotypic switching. Genetic inactivation of AMPKα2 downregulated contractile proteins while upregulating synthetic proteins in the atherosclerotic plaques and in isolated VSMC. Mechanistically, this phenotype is attributable to NF-κB activation induced transcriptional upregulation of KLF4 in VSMC. Consistently, genetic or pharmacological inhibition of either KLF4 or NF-κB ablated VSMC phenotypic switching in cultured VSMC. Further, our study suggests that AMPKα2 deletion promotes the features of atherosclerotic plaque instability. VSMC-specific *AMPKα2*$^{-/-}$ mice exhibited aggravated VSMC phenotypic switching and obvious features of plaque instability. Importantly, pravastatin treatment significantly suppressed VSMC phenotypic switching and enhanced plaque stability in *Apoe*$^{-/-}$*AMPKα2sm*$^{+/+}$ control mice but had no effect in VSMC-specific *AMPKα2*$^{-/-}$ mice. These results imply that AMPKα2 play a protective role in regulating VSMC phenotypic switching and plaque stability.

The major finding of this study is that AMPKα2 deletion in VSMC enhances atherosclerotic plaque instability. Accumulating evidence indicate that AMPK acts as an important regulator in the pathogenesis of cardiovascular diseases[40]. In our present study, we found that genetic inactivation of AMPKα2 promotes features of unstable plaques in advanced western diet-induced atherosclerotic lesions within the BA. We further confirmed our findings using VSMC-specific *AMPKα2*$^{-/-}$ mice, which displayed similar features of plaque instability in the BA to that of global *AMPKα2*$^{-/-}$ mice. Those data indicate that VSMC-derived AMPKα2, even as a minor isoform, does play an important protective role in plaque stabilization.

Another major finding of this study is we demonstrate that AMPKα2 deletion promotes VSMC phenotypic switching in a NF-κB-KLF4 dependent manner. KLF4 has been reported to function as a critical regulator in atherosclerosis[8, 41]. However, the regulation of KLF4 is still not fully understood. Accumulated evidence suggests that KLF4 can be transcriptionally induced in macrophages, VSMC, and other cell types of the vessel in response to vascular injury[42, 43]. In addition, KLF4 activity may also be regulated by post-translational modifications including acetylation, phosphorylation, and sumoylation[44–46]. Here in the present study, we demonstrate that AMPKα2 deficiency activates the NF-κB pathway in VSMC, which is consistent with our previous studies in endothelial cells[18]. Importantly, we report for the first time that NF-κB p65 binds with KLF4 promoter and transcriptionally regulates its expression, which provide a novel mechanism for KLF4 regulation in VSMC. Evidence demonstrates that many transcriptional regulatory pathways, including but not limited to SRF, Myocardin, KLF4, and FoxO4 control VSMC switching from a contractile to synthetic phenotype[47, 48]. In our study, we found that AMPKα2 deficiency enhanced VSMC phenotypic switching via upregulating KLF4.

Our results provide a novel role of AMPKα2 as a strong negative regulator in VSMC phenotypic switching. Consistent with the strong secretion character of synthetic VSMC, we observed significantly increased extracellular matrix such as collagen I and collagen IV in *AMPKα2*$^{-/-}$ VSMC compared with those in WT. Meanwhile, MMP2 expression and MMP2 activity were also markedly elevated in *AMPKα2*$^{-/-}$ VSMC when compared to those in WT (Supplemental Figure IXA). Since MMPs can degrade collagen, the levels of collagen in vascular tissues is determined by the rates of its de novo synthesis and MMP2 degradation. The MMPs-mediated collagen degradation appears to output de novo collagen synthesis in *AMPKα2*$^{-/-}$ VSMC, as the levels of collagen contents in the atherosclerotic plaque of *Apoe*$^{-/-}$*AMPKα2*$^{-/-}$ mice is lower than those in *Apoe*$^{-/-}$ mice (Figure 1 I and J). VSMC deletion of AMPKα2 promotes KLF-mediated VSMC phenotypic switching resulting in decrease of collagen and reduced plaque stability. Over all, our study support the notion that selective AMPKα2 activation in VSMC might be an effective therapy for treating unstable coronary heart diseases.

Accumulating studies have reported that statins can reduce the risk of acute coronary syndrome caused by plaque rupture[6], however, the mechanism is still unclear. It has been reported that pravastatin could increase plaque stability and inhibit thrombosis through both lipid-dependent and lipid-independent way. Recently, increasing evidence demonstrates that statins have potent anti-inflammation effects that contribute to atherosclerotic plaque

stabilization[49]. In our study, 50 mg/kg/day pravastatin was used for the treatment of plaque instability. This dose was chosen according to the guideline of pravastatin sodium tablets, in which illustrates that 100 mg/kg/day dose produces drug exposures approximately 2 times the human dose of 80 mg based on AUC. In addition, several groups have verified that 50 mg/kg/day pravastatin is an appropriate dose for preventing cardiovascular disease and renal ischemia reperfusion injury in mouse model[50, 51]. We found that 4 weeks treatment with pravastatin alleviates western diet-induced plaque instability in advanced atherosclerosis, which is consistent with previous studies reporting the beneficial effect of statins on plaque stability[27, 32, 52, 53]. Interestingly, pravastatin has no effect on serum cholesterol and triglyceride levels, which demonstrate that the protective effect of pravastatin on plaque stability in our study is lipid-independent. Consistent with early reports that statin activated AMPK in mice endothelial cells[37], we found that pravastatin efficiently activated AMPK in VSMC and in aorta from western diet treated mice (Figure 4A and 4B). However, AMPK activation in endothelial cells reported by us[37] and others[54] appears to be unrelated to statin's protective effects in plaque stability because the effect of pravastatin on plaque stability was abolished in VSMC-specific AMPKα2$^{-/-}$ mice. These data indicate that pravastatin enhances plaque stability via directly activating VSMC-derived AMPKα2. These findings suggest that AMPKα2, especially VSMC-derived AMPKα2, is an attractive therapeutic target for enhancing atherosclerotic plaque stability in clinical practice. As would be expected, AMPKα2 agonist, especially VSMC-specific AMPKα2 agonist may have direct beneficial effect on prevention of atherosclerotic plaque instability. This finding holds promise in leading to effective preventive and therapeutic strategies for vascular diseases.

Because rupture of the atherosclerotic plaque is hard to study directly in humans, it is important to use mouse model to understand how rupture occurs and explore novel therapeutic measures to prevent it from happening. The BA has been reported as the only site in high fat diet fed mouse which could display multiple features of plaque instability[32]. However, this model only partially mimics the features of unstable plaque in humans, likely due to its lack of thrombosis formation in mice[23]. In addition, the BA is very small and consequently difficult to process for histology. Until now, there has been no ideal mouse model of human plaque rupture, hence, we focused on BA for studying plaque vulnerability in terms of an advanced atherosclerotic lesion as a useful mouse model.

In conclusion, results of the present study provide evidence that AMPKα2 plays a protective role in suppressing VSMC phenotypic switching and enhancing plaque stability in advanced atherosclerosis. This novel finding provides rationale for AMPKα2 as a potential therapeutic target in preventing atherosclerotic plaque instability.

Supplementary Material

Refer to Web version on PubMed Central for supplementary material.

Acknowledgments

SOURCES OF FUNDING

This study was supported by grants from the National Institutes of Heart, Lungs, and Blood and National Institute of Aging.

Nonstandard Abbreviations and Acronyms:

AMPK	AMP-activated protein kinase
VSMC	Vascular smooth muscle cells
HASMC	Human aortic smooth muscle cell
BA	brachiocephalic arteries
KLF4	Kruppel-like factor 4
ChIP	Chromatin immunoprecipitation
IHC	Immunohistochemistry
IF	Immunofluorescence

REFERENCES

1. Lusis AJ. Atherosclerosis. Nature. 2000;407:233–241 [PubMed: 11001066]
2. Hansson GK. Inflammation, atherosclerosis, and coronary artery disease. N Engl J Med. 2005;352:1685–1695 [PubMed: 15843671]
3. Yla-Herttuala S, Bentzon JF, Daemen M, Falk E, Garcia-Garcia HM, Herrmann J, Hoefer I, Jukema JW, Krams R, Kwak BR, Marx N, Naruszewicz M, Newby A, Pasterkamp G, Serruys PW, Waltenberger J, Weber C, Tokgozoglu L. Stabilisation of atherosclerotic plaques. Position paper of the european society of cardiology (esc) working group on atherosclerosis and vascular biology. Thromb Haemost. 2011;106:1–19 [PubMed: 21670845]
4. Rzucidlo EM, Martin KA, Powell RJ. Regulation of vascular smooth muscle cell differentiation. J Vasc Surg. 2007;45 Suppl A:A25–32 [PubMed: 17544021]
5. Bennett MR. Apoptosis of vascular smooth muscle cells in vascular remodelling and atherosclerotic plaque rupture. Cardiovasc Res. 1999;41:361–368 [PubMed: 10341835]
6. Clarke M, Bennett M. Defining the role of vascular smooth muscle cell apoptosis in atherosclerosis. Cell Cycle. 2006;5:2329–2331 [PubMed: 17012894]
7. Clarke MC, Figg N, Maguire JJ, Davenport AP, Goddard M, Littlewood TD, Bennett MR. Apoptosis of vascular smooth muscle cells induces features of plaque vulnerability in atherosclerosis. Nat Med. 2006;12:1075–1080 [PubMed: 16892061]
8. Shankman LS, Gomez D, Cherepanova OA, Salmon M, Alencar GF, Haskins RM, Swiatlowska P, Newman AA, Greene ES, Straub AC, Isakson B, Randolph GJ, Owens GK. Klf4-dependent phenotypic modulation of smooth muscle cells has a key role in atherosclerotic plaque pathogenesis. Nat Med. 2015;21:628–637 [PubMed: 25985364]
9. Davies SP, Hawley SA, Woods A, Carling D, Haystead TA, Hardie DG. Purification of the amp-activated protein kinase on atp-gamma-sepharose and analysis of its subunit structure. Eur J Biochem. 1994;223:351–357 [PubMed: 8055903]
10. Mitchelhill KI, Stapleton D, Gao G, House C, Michell B, Katsis F, Witters LA, Kemp BE. Mammalian amp-activated protein kinase shares structural and functional homology with the catalytic domain of yeast snf1 protein kinase. J Biol Chem. 1994;269:2361–2364 [PubMed: 7905477]
11. Gao G, Fernandez CS, Stapleton D, Auster AS, Widmer J, Dyck JR, Kemp BE, Witters LA. Non-catalytic beta- and gamma-subunit isoforms of the 5'-amp-activated protein kinase. J Biol Chem. 1996;271:8675–8681 [PubMed: 8621499]

12. Stapleton D, Mitchelhill KI, Gao G, Widmer J, Michell BJ, Teh T, House CM, Fernandez CS, Cox T, Witters LA, Kemp BE. Mammalian amp-activated protein kinase subfamily. J Biol Chem. 1996;271:611–614 [PubMed: 8557660]
13. Viollet B, Horman S, Leclerc J, Lantier L, Foretz M, Billaud M, Giri S, Andreelli F. Ampk inhibition in health and disease. Crit Rev Biochem Mol Biol. 2010;45:276–295 [PubMed: 20522000]
14. Braco JT, Gillespie EL, Alberto GE, Brenman JE, Johnson EC. Energy-dependent modulation of glucagon-like signaling in drosophila via the amp-activated protein kinase. Genetics. 2012;192:457–466 [PubMed: 22798489]
15. Li Y, Xu S, Mihaylova MM, Zheng B, Hou X, Jiang B, Park O, Luo Z, Lefai E, Shyy JY, Gao B, Wierzbicki M, Verbeuren TJ, Shaw RJ, Cohen RA, Zang M. Ampk phosphorylates and inhibits srebp activity to attenuate hepatic steatosis and atherosclerosis in diet-induced insulin-resistant mice. Cell Metab. 2011;13:376–388 [PubMed: 21459323]
16. Motoshima H, Goldstein BJ, Igata M, Araki E. Ampk and cell proliferation--ampk as a therapeutic target for atherosclerosis and cancer. J Physiol. 2006;574:63–71 [PubMed: 16613876]
17. Dong Y, Zhang M, Liang B, Xie Z, Zhao Z, Asfa S, Choi HC, Zou MH. Reduction of amp-activated protein kinase alpha2 increases endoplasmic reticulum stress and atherosclerosis in vivo. Circulation. 2010;121:792–803 [PubMed: 20124121]
18. Wang S, Zhang M, Liang B, Xu J, Xie Z, Liu C, Viollet B, Yan D, Zou MH. Ampkalpha2 deletion causes aberrant expression and activation of nad(p)h oxidase and consequent endothelial dysfunction in vivo: Role of 26s proteasomes. Circ Res. 2010;106:1117–1128 [PubMed: 20167927]
19. Song P, Wang S, He C, Liang B, Viollet B, Zou MH. Ampkalpha2 deletion exacerbates neointima formation by upregulating skp2 in vascular smooth muscle cells. Circulation research. 2011;109:1230–1239 [PubMed: 21980125]
20. Song P, Zhou Y, Coughlan KA, Dai X, Xu H, Viollet B, Zou MH. Adenosine monophosphate-activated protein kinase-alpha2 deficiency promotes vascular smooth muscle cell migration via s-phase kinase-associated protein 2 upregulation and e-cadherin downregulation. Arterioscler Thromb Vasc Biol. 2013;33:2800–2809 [PubMed: 24115035]
21. Takaya N, Yuan C, Chu B, Saam T, Polissar NL, Jarvik GP, Isaac C, McDonough J, Natiello C, Small R, Ferguson MS, Hatsukami TS. Presence of intraplaque hemorrhage stimulates progression of carotid atherosclerotic plaques: A high-resolution magnetic resonance imaging study. Circulation. 2005;111:2768–2775 [PubMed: 15911695]
22. Kolodgie FD, Gold HK, Burke AP, Fowler DR, Kruth HS, Weber DK, Farb A, Guerrero LJ, Hayase M, Kutys R, Narula J, Finn AV, Virmani R. Intraplaque hemorrhage and progression of coronary atheroma. N Engl J Med. 2003;349:2316–2325 [PubMed: 14668457]
23. Jackson CL, Bennett MR, Biessen EA, Johnson JL, Krams R. Assessment of unstable atherosclerosis in mice. Arterioscler Thromb Vasc Biol. 2007;27:714–720 [PubMed: 17332492]
24. Burke AP, Kolodgie FD, Farb A, Weber DK, Malcom GT, Smialek J, Virmani R. Healed plaque ruptures and sudden coronary death: Evidence that subclinical rupture has a role in plaque progression. Circulation. 2001;103:934–940 [PubMed: 11181466]
25. Finn AV, Nakano M, Narula J, Kolodgie FD, Virmani R. Concept of vulnerable/unstable plaque. Arterioscler Thromb Vasc Biol. 2010;30:1282–1292 [PubMed: 20554950]
26. Neumeister V, Scheibe M, Lattke P, Jaross W. Determination of the cholesterol-collagen ratio of arterial atherosclerotic plaques using near infrared spectroscopy as a possible measure of plaque stability. Atherosclerosis. 2002;165:251–257 [PubMed: 12417275]
27. Crisby M, Nordin-Fredriksson G, Shah PK, Yano J, Zhu J, Nilsson J. Pravastatin treatment increases collagen content and decreases lipid content, inflammation, metalloproteinases, and cell death in human carotid plaques: Implications for plaque stabilization. Circulation. 2001;103:926–933 [PubMed: 11181465]
28. Davies MJ, Richardson PD, Woolf N, Katz DR, Mann J. Risk of thrombosis in human atherosclerotic plaques: Role of extracellular lipid, macrophage, and smooth muscle cell content. Br Heart J. 1993;69:377–381 [PubMed: 8518056]

29. Libby P, Geng YJ, Aikawa M, Schoenbeck U, Mach F, Clinton SK, Sukhova GK, Lee RT. Macrophages and atherosclerotic plaque stability. Curr Opin Lipidol. 1996;7:330–335 [PubMed: 8937525]
30. Michel JB, Virmani R, Arbustini E, Pasterkamp G. Intraplaque haemorrhages as the trigger of plaque vulnerability. Eur Heart J. 2011;32:1977–1985, 1985a, 1985b, 1985c [PubMed: 21398643]
31. Mann J, Davies MJ. Mechanisms of progression in native coronary artery disease: Role of healed plaque disruption. Heart. 1999;82:265–268 [PubMed: 10455072]
32. Johnson J, Carson K, Williams H, Karanam S, Newby A, Angelini G, George S, Jackson C. Plaque rupture after short periods of fat feeding in the apolipoprotein e-knockout mouse: Model characterization and effects of pravastatin treatment. Circulation. 2005;111:1422–1430 [PubMed: 15781753]
33. Virmani R, Burke AP, Kolodgie FD, Farb A. Vulnerable plaque: The pathology of unstable coronary lesions. J Interv Cardiol. 2002;15:439–446 [PubMed: 12476646]
34. Yla-Herttuala S, Bentzon JF, Daemen M, Falk E, Garcia-Garcia HM, Herrmann J, Hoefer I, Jauhiainen S, Jukema JW, Krams R, Kwak BR, Marx N, Naruszewicz M, Newby A, Pasterkamp G, Serruys PW, Waltenberger J, Weber C, Tokgozoglu L, Atherosclerosis ESCWGo, Vascular B. Stabilization of atherosclerotic plaques: An update. Eur Heart J. 2013;34:3251–3258 [PubMed: 23966311]
35. Salabei JK, Cummins TD, Singh M, Jones SP, Bhatnagar A, Hill BG. Pdgf-mediated autophagy regulates vascular smooth muscle cell phenotype and resistance to oxidative stress. Biochem J. 2013;451:375–388 [PubMed: 23421427]
36. El-Karim EA, Hagos EG, Ghaleb AM, Yu B, Yang VW. Kruppel-like factor 4 regulates genetic stability in mouse embryonic fibroblasts. Mol Cancer. 2013;12:89 [PubMed: 23919723]
37. Choi HC, Song P, Xie Z, Wu Y, Xu J, Zhang M, Dong Y, Wang S, Lau K, Zou MH. Reactive nitrogen species is required for the activation of the amp-activated protein kinase by statin in vivo. J Biol Chem. 2008;283:20186–20197 [PubMed: 18474592]
38. Hwang JT, Ha J, Park OJ. Combination of 5-fluorouracil and genistein induces apoptosis synergistically in chemo-resistant cancer cells through the modulation of ampk and cox-2 signaling pathways. Biochem Biophys Res Commun. 2005;332:433–440 [PubMed: 15896711]
39. Leverve XM, Guigas B, Detaille D, Batandier C, Koceir EA, Chauvin C, Fontaine E, Wiernsperger NF. Mitochondrial metabolism and type-2 diabetes: A specific target of metformin. Diabetes Metab. 2003;29:6S88–94 [PubMed: 14502105]
40. Shirwany NA, Zou MH. Ampk in cardiovascular health and disease. Acta Pharmacol Sin. 2010;31:1075–1084 [PubMed: 20711221]
41. Yan FF, Liu YF, Liu Y, Zhao YX. Klf4: A novel target for the treatment of atherosclerosis. Medical hypotheses. 2008;70:845–847 [PubMed: 17869009]
42. Zheng X, Li A, Zhao L, Zhou T, Shen Q, Cui Q, Qin X. Key role of microrna-15a in the klf4 suppressions of proliferation and angiogenesis in endothelial and vascular smooth muscle cells. Biochem Biophys Res Commun. 2013;437:625–631 [PubMed: 23867820]
43. Sharma N, Lu Y, Zhou G, Liao X, Kapil P, Anand P, Mahabeleshwar GH, Stamler JS, Jain MK. Myeloid kruppel-like factor 4 deficiency augments atherogenesis in apoe−/− mice--brief report. Arterioscler Thromb Vasc Biol. 2012;32:2836–2838 [PubMed: 23065827]
44. Li HX, Han M, Bernier M, Zheng B, Sun SG, Su M, Zhang R, Fu JR, Wen JK. Kruppel-like factor 4 promotes differentiation by transforming growth factor-beta receptor-mediated smad and p38 mapk signaling in vascular smooth muscle cells. J Biol Chem. 2010;285:17846–17856 [PubMed: 20375011]
45. Evans PM, Zhang W, Chen X, Yang J, Bhakat KK, Liu C. Kruppel-like factor 4 is acetylated by p300 and regulates gene transcription via modulation of histone acetylation. J Biol Chem. 2007;282:33994–34002 [PubMed: 17908689]
46. Tahmasebi S, Ghorbani M, Savage P, Yan K, Gocevski G, Xiao L, You L, Yang XJ. Sumoylation of kruppel-like factor 4 inhibits pluripotency induction but promotes adipocyte differentiation. J Biol Chem. 2013;288:12791–12804 [PubMed: 23515309]
47. Mack CP. Signaling mechanisms that regulate smooth muscle cell differentiation. Arterioscler Thromb Vasc Biol. 2011;31:1495–1505 [PubMed: 21677292]

48. Spin JM, Maegdefessel L, Tsao PS. Vascular smooth muscle cell phenotypic plasticity: Focus on chromatin remodelling. Cardiovascular research. 2012;95:147–155 [PubMed: 22362814]

49. Jain MK, Ridker PM. Anti-inflammatory effects of statins: Clinical evidence and basic mechanisms. Nat Rev Drug Discov. 2005;4:977–987 [PubMed: 16341063]

50. Sharyo S, Yokota-Ikeda N, Mori M, Kumagai K, Uchida K, Ito K, Burne-Taney MJ, Rabb H, Ikeda M. Pravastatin improves renal ischemia-reperfusion injury by inhibiting the mevalonate pathway. Kidney Int. 2008;74:577–584 [PubMed: 18509318]

51. McLoughlin D, McGuinness J, Byrne J, Terzo E, Huuskonen V, McAllister H, Black A, Kearney S, Kay E, Hill ADK, Dietz HC, Redmond JM. Pravastatin reduces marfan aortic dilation. Circulation. 2011;124:S168–S173 [PubMed: 21911808]

52. Watanabe K, Sugiyama S, Kugiyama K, Honda O, Fukushima H, Koga H, Horibata Y, Hirai T, Sakamoto T, Yoshimura M, Yamashita Y, Ogawa H. Stabilization of carotid atheroma assessed by quantitative ultrasound analysis in nonhypercholesterolemic patients with coronary artery disease. Journal of the American College of Cardiology. 2005;46:2022–2030 [PubMed: 16325036]

53. Libby P. Collagenases and cracks in the plaque. The Journal of clinical investigation. 2013;123:3201–3203 [PubMed: 23908120]

54. Sun W, Lee TS, Zhu M, Gu C, Wang Y, Zhu Y, Shyy JY. Statins activate amp-activated protein kinase in vitro and in vivo. Circulation. 2006;114:2655–2662 [PubMed: 17116771]

Novelty and Significance

What Is Known?

- Atherosclerotic plaque rupture leading to intra-luminal obstructive thrombosis is the most important cause for acute coronary syndromes.
- The AMP-activated protein kinase (AMPK) has been reported to play a protective role in atherosclerosis.
- Statins have been reported to increase plaque stability and reduce the risk of acute coronary syndrome.
- KLF4 is a well-known regulator for VSMC phenotypic switch. Deletion of the *Klf4* gene increases plaque stability.

What New Information Does This Article Contribute?

- AMPKα2 deficiency in VSMC enhances diet-induced atherosclerotic plaque instability in vivo.
- Administration of pravastatin prevents diet-induced VSMC phenotypic switch and atherosclerotic plaque instability via activation of AMPKα2 in vivo.
- AMPKα2 deficiency promotes VSMC phenotypic switch and atherosclerotic plaque instability via upregulating KLF4.
- AMPKα2 deletion activates NF-κB pathway, transcriptionally upregulates KLF4, leading to VSMC phenotypic switch, and atherosclerotic plaque instability.

Rupture of atherosclerotic plaque is the major cause of morbidity and mortality in the world. Our study shows that loss of AMPKα2 in VSMC promotes VSMC phenotypic switch and enhances atherosclerotic plaque instability. Pravastatin treatment markedly prevented diet-induced atherosclerotic plaque instability by activating AMPKα2 in VSMCs. The findings identify AMPKα2 as a potential therapeutic target in preventing atherosclerotic plaque instability.

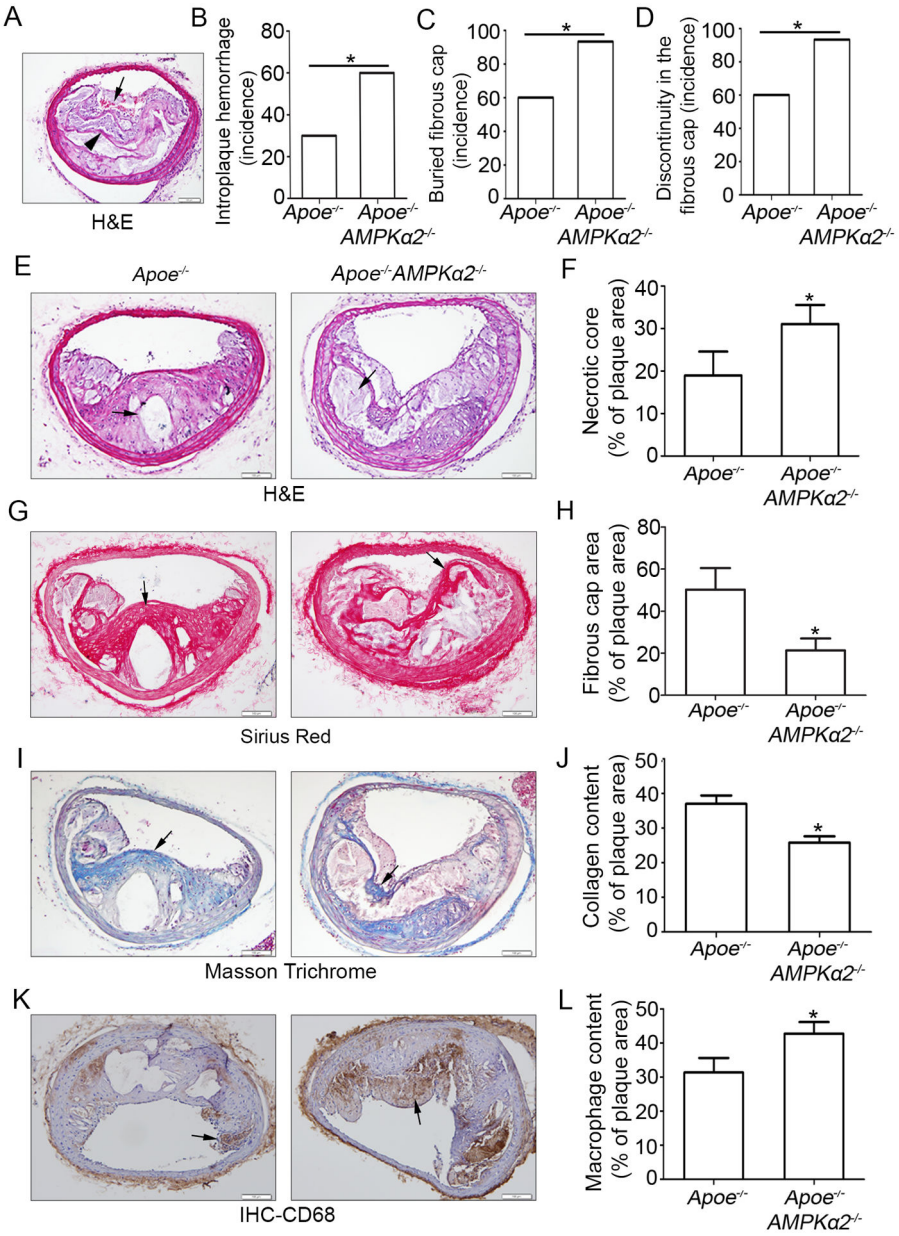

Figure 1. AMPKα2 deletion enhances western diet-induced features of atherosclerotic plaque instability in the BA.

(A) Representative images from BA lesions of *Apoe*$^{-/-}$ and *Apoe*$^{-/-}$*AMPKα2*$^{-/-}$ mice with H&E staining for intraplaque hemorrhage (black arrow) and buried fibrous cap (black arrowhead). (B-D) Incidence for intraplaque hemorrhage (B), presence of buried fibrous cap (C) and presence of fibrous cap discontinuity (D) in the BA of *Apoe*$^{-/-}$ and *Apoe*$^{-/-}$*AMPKα2*$^{-/-}$ mice. (E-F) Representative images and quantification of necrotic core area in the BA based on H&E staining (black arrow) of *Apoe*$^{-/-}$ and *Apoe*$^{-/-}$*AMPKα2*$^{-/-}$ mice. (G-H) Representative images and quantification for the area of fibrous cap staining (black line) in BA based on Sirius Red staining (red staining) of *Apoe*$^{-/-}$ and *Apoe*$^{-/-}$*AMPKα2*$^{-/-}$ mice. (I-J) Representative images and quantification of plaque collagen content in BA based on Masson trichrome staining (Blue staining, black arrow)) of *Apoe*$^{-/-}$ and *Apoe*

$^{-/-}AMPK\alpha 2^{-/-}$ mice. (K-L) Representative images and quantification of plaque macrophage content in BA based on CD68 IHC staining (Brown staining, black arrow)) of $Apoe^{-/-}$ and $Apoe^{-/-}AMPK\alpha 2^{-/-}$ mice. n=20–21 in each group. Values represent the mean ± SEM. *, P<0.05 vs. $Apoe^{-/-}$ mice. Scale bar=100 μm.

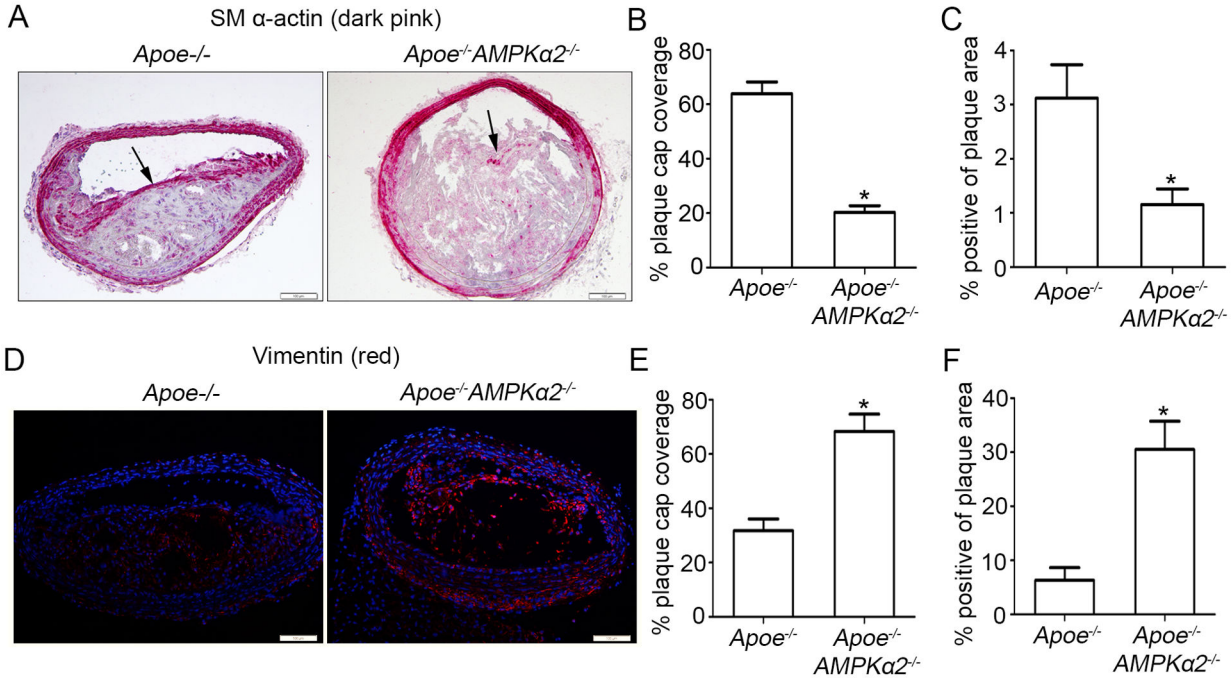

Figure 2. AMPKα2 deletion induces VSMC phenotypic switching in advanced atherosclerotic plaque in the BA.

(A) Representative images of IHC staining of SM α-actin (dark pink) in BA of *Apoe*$^{-/-}$ and *Apoe*$^{-/-}$*AMPKα2*$^{-/-}$ mice. Arrow represents representative staining of SM α-actin. Scale bar=100 μm. (B) Quantification of plaque SM α-actin coverage on the plaque cap in BA of *Apoe*$^{-/-}$ and *Apoe*$^{-/-}$*AMPKα2*$^{-/-}$ mice. (C) Quantification of total plaque SM α-actin content in BA of *Apoe*$^{-/-}$ and *Apoe*$^{-/-}$*AMPKα2*$^{-/-}$ mice. (D) Representative images of IF staining of vimentin (red) in BA of *Apoe*$^{-/-}$ and *Apoe*$^{-/-}$*AMPKα2*$^{-/-}$ mice. Dapi = blue staining of nucleus. Scale bar=100 μm. (E) Quantification of plaque vimentin coverage on the plaque cap in BA of *Apoe*$^{-/-}$ and *Apoe*$^{-/-}$*AMPKα2*$^{-/-}$ mice. (F) Quantification of total plaque vimentin content in BA of *Apoe*$^{-/-}$ and *Apoe*$^{-/-}$*AMPKα2*$^{-/-}$ mice. n=10 in each group. Values represent the mean ± SEM. *, P<0.05 vs. *Apoe*$^{-/-}$ *mice.*

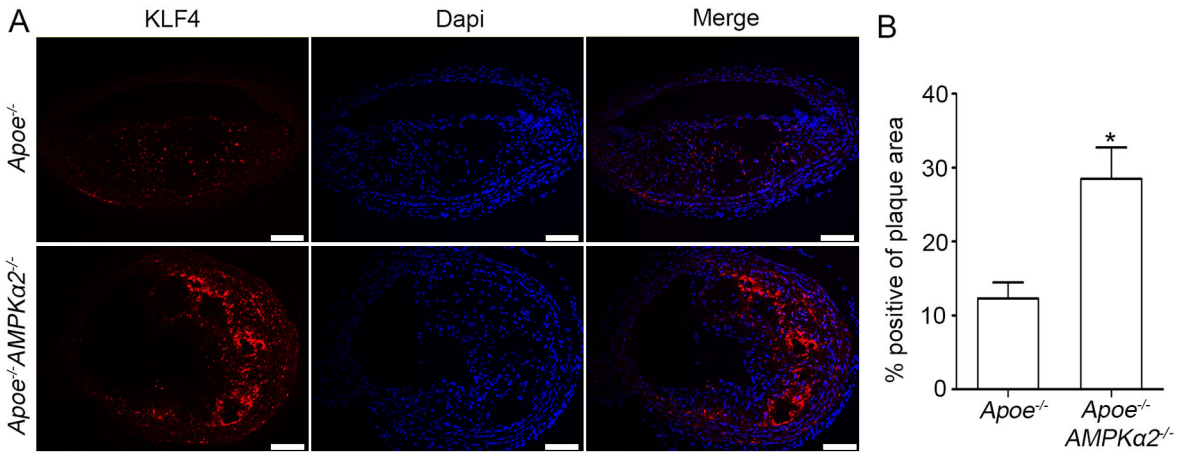

Figure 3. AMPKα2 deletion upregulates KLF4 expression in advanced atherosclerotic plaque in the BA.

(A) IF staining of KLF4 (red) in BA of *Apoe*$^{-/-}$ and *Apoe*$^{-/-}$*AMPKα2*$^{-/-}$ mice. Dapi = blue staining of nucleus. Scale bar=100 μm. (B) Quantification of KLF4 expression in BA of *Apoe*$^{-/-}$ and *Apoe*$^{-/-}$*AMPKα2*$^{-/-}$ mice. n=10 in each group. Values represent the mean ± SEM. *, P<0.05 vs. *Apoe*$^{-/-}$ mice.

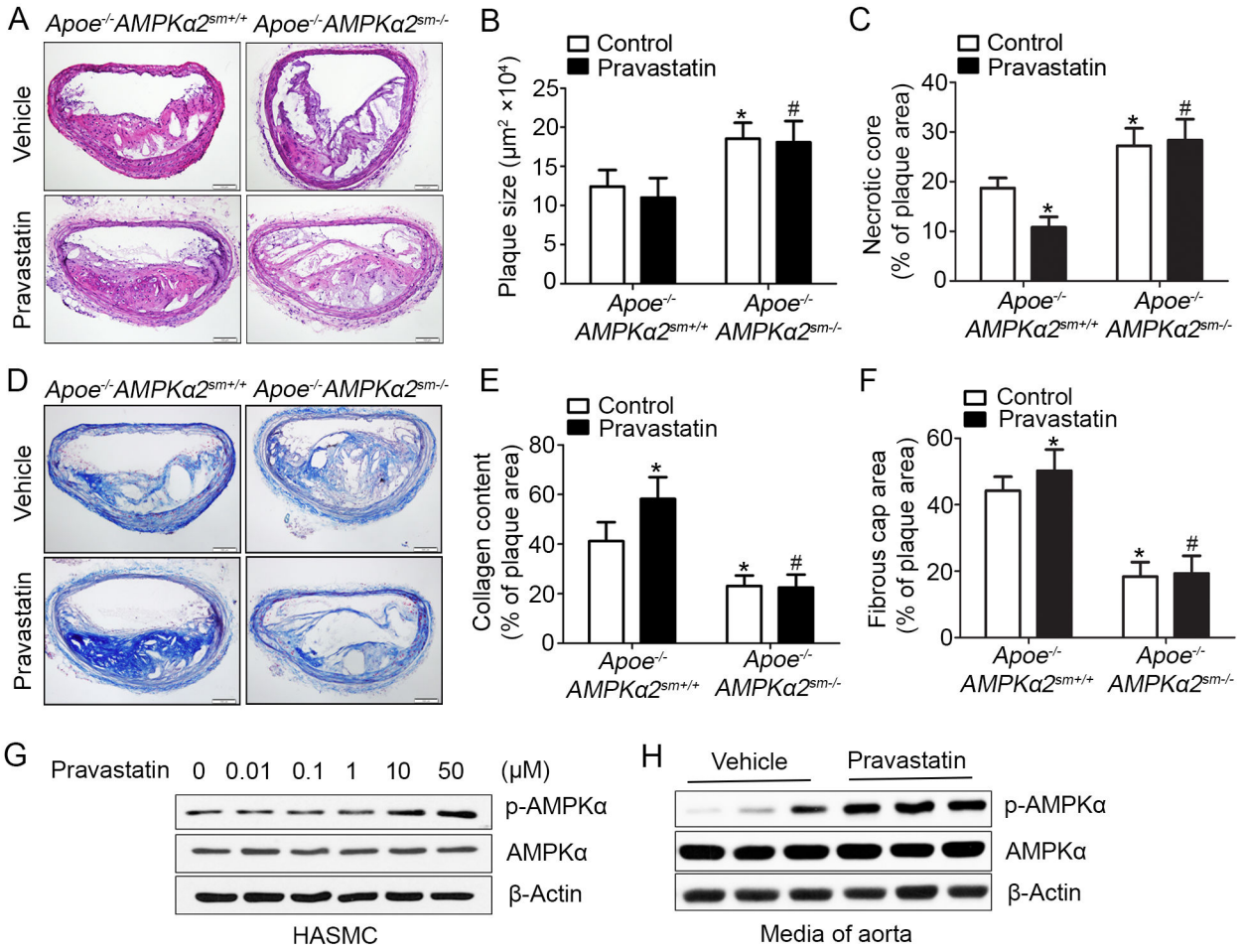

Figure 4. Pravastatin treatment alleviates western diet-induced plaque instability in *Apoe*$^{-/-}$*AMPKα2*$^{sm+/+}$ mice, but not in *Apoe*$^{-/-}$*AMPKα2*$^{sm-/-}$ mice.

(A) Representative images from H&E staining of the BA in *Apoe*$^{-/-}$*AMPKα2*$^{sm+/+}$ and *Apoe*$^{-/-}$*AMPKα2*$^{sm-/-}$ mice treated with or without pravastatin. Scale bar=100 μm. (B) Quantification of plaque size and (C) necrotic core size in the BA of *Apoe*$^{-/-}$*AMPKα2*$^{sm+/+}$ and *Apoe*$^{-/-}$*AMPKα2*$^{sm-/-}$ mice treated with or without pravastatin. (D-E) Representative images and quantification of plaque collagen content in the BA based on Masson trichrome staining of *Apoe*$^{-/-}$*AMPKα2*$^{sm+/+}$ and *Apoe*$^{-/-}$*AMPKα2*$^{sm-/-}$ mice treated with or without pravastatin. Scale bar=100 μm. (F) Quantification of fibrous cap area in the BA of *Apoe*$^{-/-}$*AMPKα2*$^{sm+/+}$ and *Apoe*$^{-/-}$*AMPKα2*$^{sm-/-}$ mice treated with or without pravastatin. n=10 in each group. Values represent the means ± SEM. *, P<0.05 vs. *Apoe*$^{-/-}$*AMPKα2*$^{sm+/+}$ mice without pravastatin treatment. #, P<0.05 vs. *Apoe*$^{-/-}$*AMPKα2*$^{sm+/+}$ mice with pravastatin treatment. (G) Western blot analysis of pAMPK*α* (Thr172) in HASMC treated with 0.01–50 μM pravastatin for 24 hours. (H) Western blot analysis of pAMPK*α* (Thr172) in aorta from *Apoe*$^{-/-}$*AMPKα2*$^{sm+/+}$ mice fed with western diet for 10 weeks and treated with or without pravastatin for 4 weeks.

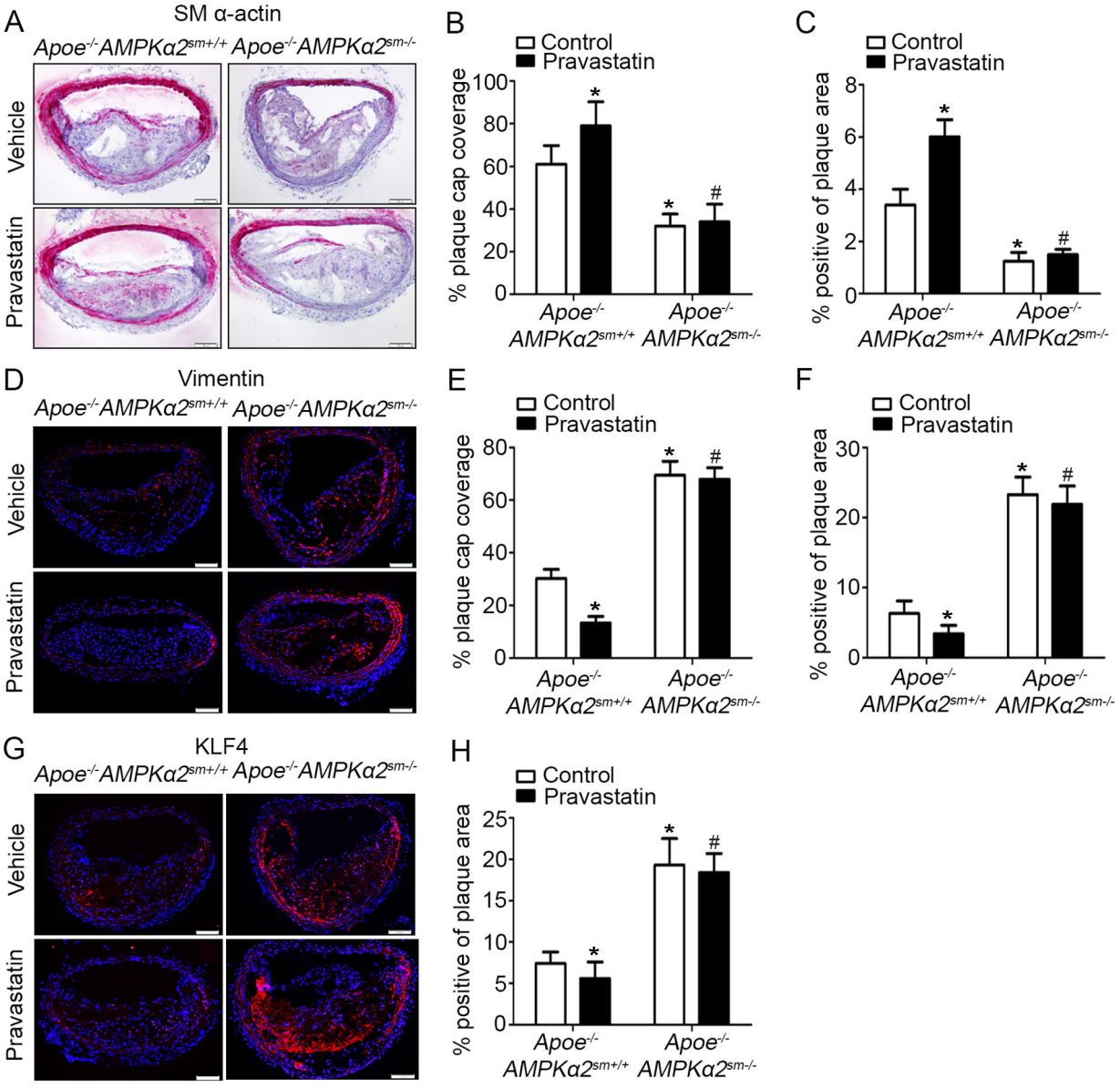

Figure 5. VSMC AMPKα2 knockdown eliminates the effect of Pravastatin treatment on VSMC phenotypic switching signaling in vivo.

(A) Representative images of IHC staining of SM α-actin (dark pink) in the BA of *Apoe*$^{-/-}$*AMPKα2*$^{sm+/+}$ and *Apoe*$^{-/-}$*AMPKα2*$^{sm-/-}$ mice treated with or without pravastatin. Scale bar=100 μm. (B-C) Quantification of plaque SM α-actin coverage on the plaque cap (B) and total plaque SM α-actin content (C) in BA of *Apoe*$^{-/-}$*AMPKα2*$^{sm+/+}$ and *Apoe*$^{-/-}$*AMPKα2*$^{sm-/-}$ mice treated with or without pravastatin. (D) Representative images of IF staining of Vimentin (red) in the BA of *Apoe*$^{-/-}$*AMPKα2*$^{sm+/+}$ and *Apoe*$^{-/-}$*AMPKα2*$^{sm-/-}$ mice treated with or without pravastatin. Dapi = blue staining of nucleus. Scale bar=100 μm (E-F) Quantification of plaque vimentin coverage on the plaque cap (E) and total plaque vimentin content (F) in BA of *Apoe*$^{-/-}$*AMPKα2*$^{sm+/+}$ and *Apoe*$^{-/-}$*AMPKα2*$^{sm-/-}$ mice treated with or without pravastatin. (G) Representative images of IF staining of KLF4 (red) in the BA of *Apoe*$^{-/-}$*AMPKα2*$^{sm+/+}$ and *Apoe*$^{-/-}$*AMPKα2*$^{sm-/-}$ mice treated with or

without pravastatin. Dapi = blue staining of nucleus. Scale bar=100 μm. (H) Quantification of KLF4 expression in BA of *Apoe*$^{-/-}$*AMPKα2*$^{sm+/+}$ and *Apoe*$^{-/-}$*AMPKα2*$^{sm-/-}$ mice treated with or without pravastatin. n=10 in each group. Values represent the means ± SEM. *, P<0.05 vs. *Apoe*$^{-/-}$*AMPKα2*$^{sm+/+}$ mice without pravastatin treatment. #, P<0.05 vs. *Apoe*$^{-/-}$*AMPKα2*$^{sm+/+}$ mice with pravastatin treatment.

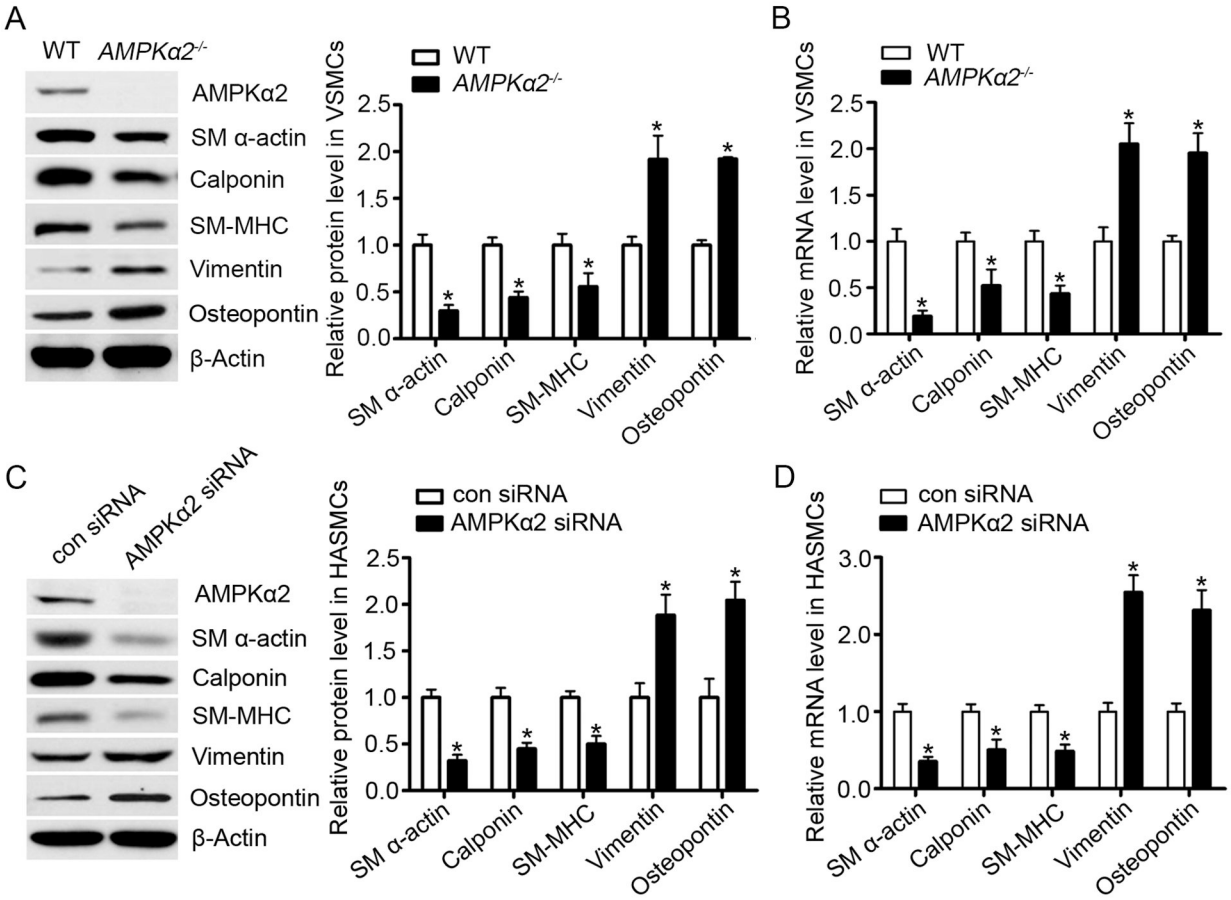

Figure 6. AMPKα2 deficiency induces VSMC phenotypic switching in vitro.

(A) Western blot analysis of contractile (SM α-actin, calponin and SM-MHC) and synthetic proteins (vimentin and osteopontin) in VSMC isolated from WT and *AMPKα2*$^{-/-}$ mice (n=5). Values represent the means ± SEM. *, P<0.05 vs. WT. (B) Quantitative real-time PCR of contractile (SM α-actin, calponin and SM-MHC) and synthetic markers (vimentin and osteopontin) in VSMC isolated from WT and *AMPKα2*$^{-/-}$ mice (n=5). Values represent the means ± SEM. *, P<0.05 vs. WT. (C) Western blot analysis of contractile and synthetic proteins in HASMC treated with con siRNA and AMPKα2 siRNA (n=5). Values represent the means ± SEM. *, P<0.05 vs. con siRNA. (D) Quantitative real-time PCR of contractile and synthetic markers in HASMC treated with con siRNA and AMPKα2 siRNA (n=5). Values represent the means ± SEM. *, P<0.05 vs. con siRNA.

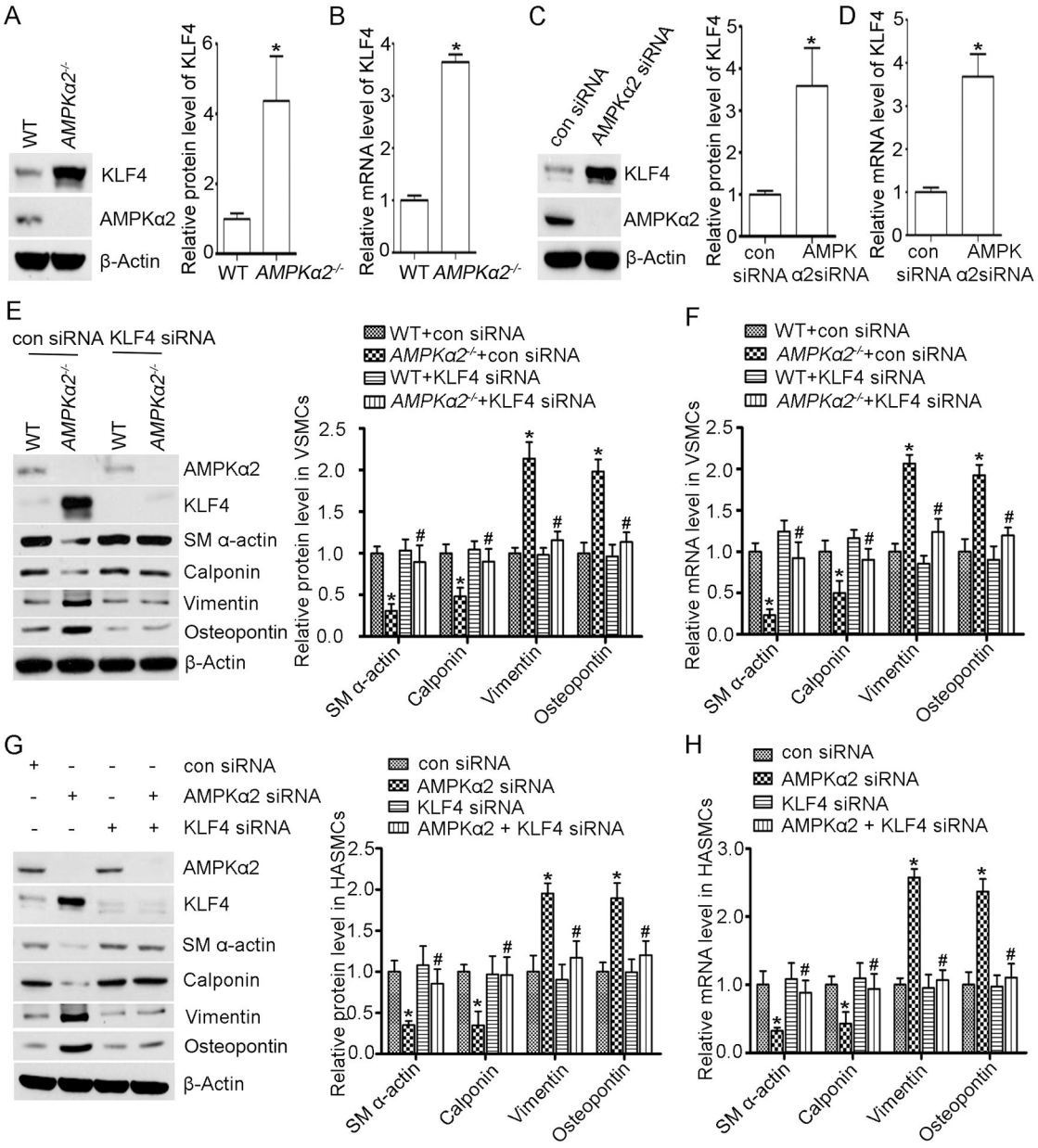

Figure 7. AMPKα2 deficiency-induced VSMC phenotype switching is in KLF4-dependent manner.

(A) Western blot analysis of KLF4 protein expression in WT and *AMPKα2*$^{-/-}$ mouse VSMC (n=5). *, P<0.05 vs. WT. (B) Quantitative real-time PCR analysis of KLF4 mRNA level in WT and *AMPKα2*$^{-/-}$ mouse VSMC (n=5). *, P<0.05 vs. WT. (C) Western blot analysis of KLF4 protein expression in HASMC treated with con siRNA and AMPKα2 siRNA (n=5). *, P<0.05 vs. con siRNA. (D) Quantitative real-time PCR analysis of KLF4 mRNA level in HASMC treated with con siRNA and AMPKα2 siRNA (n=5). *, P<0.05 vs. con siRNA. (E) Western blot analysis of protein expression of SM α-actin, calponin, vimentin and osteopontin in WT and *AMPKα2*$^{-/-}$ mouse VSMC treated with con siRNA and KLF4 siRNA for 48 hours (n=5). *, P<0.05 vs. WT+con siRNA. #, P<0.05 vs. *AMPKα2*$^{-/-}$ +con siRNA. (F) Quantitative real-time PCR analysis of mRNA level of SM α-

actin, calponin, vimentin and osteopontin in WT and *AMPKα2*$^{-/-}$ mouse VSMC treated with con siRNA and KLF4 siRNA for 48 hours (n=5). *, P<0.05 vs. WT+con siRNA. #, P<0.05 vs. *AMPKα2*$^{-/-}$ +con siRNA. (G) Western blot analysis of protein expression of SM α-actin, calponin, vimentin and osteopontin in HASMC treated with con siRNA, AMPKα2 siRNA and KLF4 siRNA for 48 hours (n=5). *, P<0.05 vs. con siRNA. #, P<0.05 vs. AMPKα2 siRNA. (H) Quantitative real-time PCR analysis of mRNA level of SM α-actin, calponin, vimentin and osteopontin in HASMC treated with con siRNA, AMPKα2 siRNA and KLF4 siRNA for 48 hours (n=5). *, P<0.05 vs. con siRNA. #, P<0.05 vs. AMPKα2 siRNA.

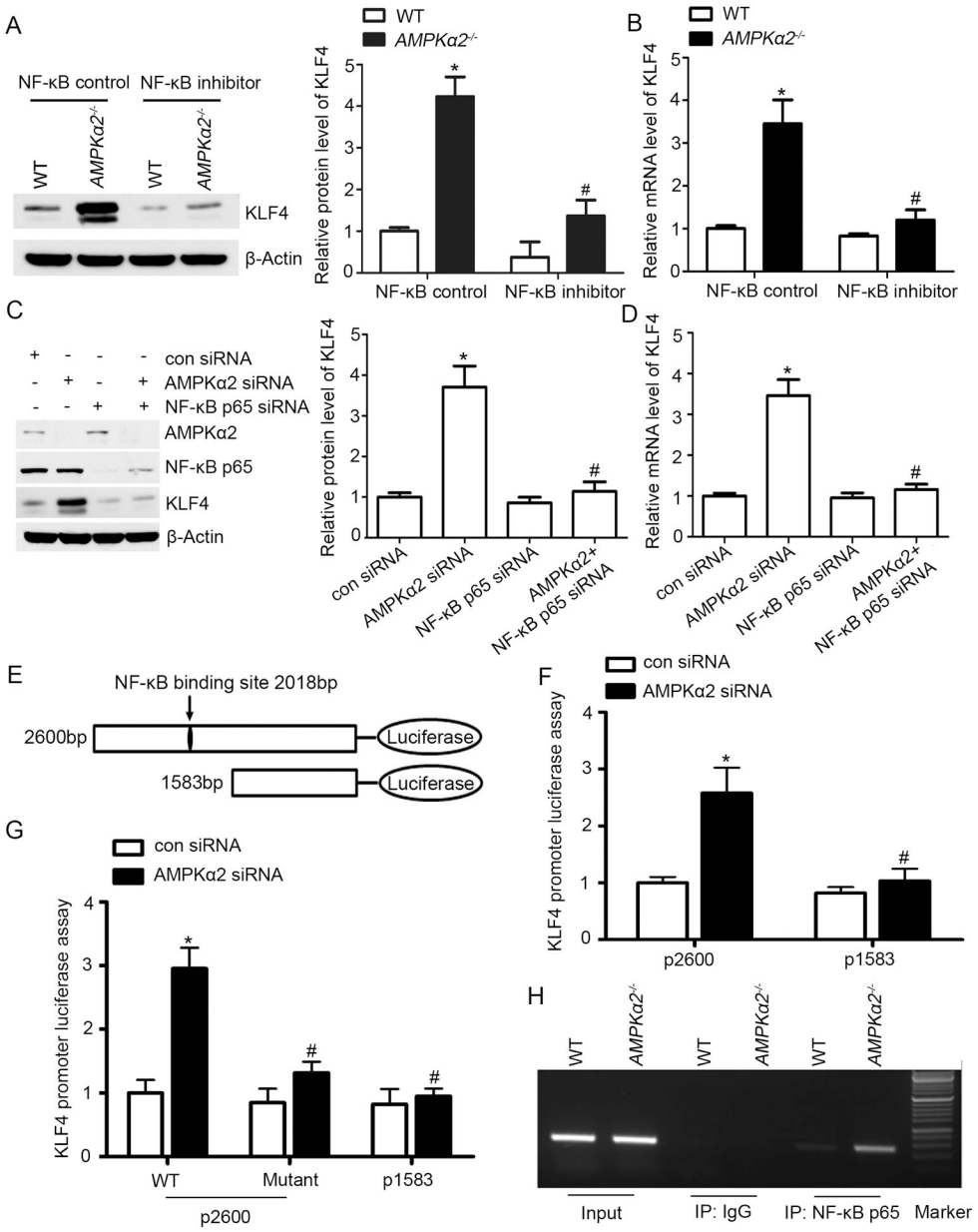

Figure 8. AMPKα2 deletion upregulates KLF4 through NF-κB signaling.

(A) Western blot analysis of KLF4 expression in WT and *AMPKα2*$^{-/-}$ mouse VSMC treated with NF-κB control and NF-κB inhibitor (n=5). *, P<0.05 vs. WT VSMC treated with NF-κB control. #, P<0.05 vs. *AMPKα2*$^{-/-}$ VSMC treated with NF-κB control. (B) Quantitative real-time PCR analysis of mRNA level of KLF4 in WT and *AMPKα2*$^{-/-}$ mouse VSMC treated with NF-κB control and NF-κB inhibitor (n=5). *, P<0.05 vs. WT VSMC treated with NF-κB control. #, P<0.05 vs. *AMPKα2*$^{-/-}$ VSMC treated with NF-κB control. (C) Western blot analysis of KLF4 expression in HASMC treated with NF-κBp65 siRNA and AMPKα2 siRNA (n=5). *, P<0.05 vs. con siRNA. #, P<0.05 vs. AMPKα2 siRNA. (D) Quantitative real-time PCR analysis of mRNA level of KLF4 in HASMC treated with NF-κBp65 siRNA and AMPKα2 siRNA (n=5). *, P<0.05 vs. con siRNA. #, P<0.05 vs.

AMPKα2 siRNA. (E) The KLF4 promoter was analyzed using the Transcription Factor Database software, suggesting one binding site within the promoter. 2,600-bp and 1,583-bp KLF4 promoter luciferase constructs are shown. (F) HASMC were transfected with 2,600-bp and 1,583-bp KLF4 promoter luciferase constructs and treated with con siRNA or AMPKα2 siRNA, and luciferase activity was measured after 24 hours. Results of the luciferase reporter assay are presented as fold changes ±SEM of the Firefly/Renilla luciferase activities (n=5). *, P<0.05 vs. HASMC transfected with 2,600-bp KLF4 promoter luciferase construct and con siRNA. #, P<0.05 vs. HASMC transfected with 2,600-bp KLF4 promoter luciferase construct and AMPKα2 siRNA. (G) HASMC were transfected with either WT or the mutant KLF4 promoter reporter and treated with con siRNA or AMPKα2 siRNA for 24 hours to detect the luciferase activity (n=5). *, P<0.05 vs. HASMC transfected with WT 2,600-bp KLF4 promoter reporter and con siRNA. #, P<0.05 vs. HASMC transfected with WT 2,600-bp KLF4 promoter reporter and AMPKα2 siRNA. (H) ChIP assay for NF-κBp65 binding with KLF4 promoter in WT and *AMPKα2*$^{-/-}$ mouse VSMC.